

Automatic micropart assembly of 3-Dimensional structure by vision based control[†]

Lidai Wang¹ and Seungmin Kim^{1,2,*}

¹*Department of Mechanical and Industrial Engineering, University of Toronto,
5 King's College Rd. Toronto, Ontario, Canada, M5S 3G8,*

²*Dept. of Mechatronics Exam., The Korean Intellectual Property Office,
#920, Dunsan-dong, Seo-gu, Daejeon, 302-701, Republic of Korea.*

(Manuscript Received February 19, 2008; Revised July 25, 2008; Accepted August 6, 2008)

Abstract

We propose a vision control strategy to perform automatic microassembly tasks in three-dimension (3-D) and develop relevant control software: specifically, using a 6 degree-of-freedom (DOF) robotic workstation to control a passive microgripper to automatically grasp a designated micropart from the chip, pivot the micropart, and then move the micropart to be vertically inserted into a designated slot on the chip. In the proposed control strategy, the whole microassembly task is divided into two subtasks, micro-grasping and micro-joining, in sequence. To guarantee the success of microassembly and manipulation accuracy, two different two-stage feedback motion strategies, the pattern matching and auto-focus method are employed, with the use of vision-based control system and the vision control software developed. Experiments conducted demonstrate the efficiency and validity of the proposed control strategy.

Keywords: MEMS; Automatic; Micro; Assembly; Vision

1. Introduction

To date, many simple microelectromechanical systems (MEMS) devices, so far, have achieved commercial success in various applications, such as inkjet printers and gyroscopes. As MEMS allows the development of smart products, augments the computational ability of microelectronics, MEMS devices become more and more complex. The need for microassembly of MEMS thus becomes apparent.

Microassembly lies between conventional (macro-scale) assembly (with part dimensions >1 mm) and the emerging field of nanoassembly (with part dimensions in the molecular scale, i.e., <1 μm). Currently, microassembly is performed largely by humans with grippers and microscopes or with high precision pick-

and-place robots. Both methods are inherently serial [1, 2], or called serial microassembly. To achieve serial microassembly, a series of sub-tasks, such as grasping a micropart with a microgripper, manipulating the micropart, and joining the part to other microstructures, etc., must be completed in a sequential process [3]. Since this microassembly approach allows for the translation and orientation of individual micropart with 6 DOF, it is used to create complex microstructures [4]. In contrast to serial microassembly, approaches of parallel microassembly and self microassembly have been proposed. The former assembles microstructures at multiple assembly sites simultaneously [5], while the latter assembles multiple microparts spontaneously under the influence of an external force such as magnetism, heat or centrifugal force [6].

Considering the features of the three microassembly approaches and the tendency of building complicated MEMS devices, serial microassembly accounts

[†] This paper was recommended for publication in revised form by Associate Editor Dong Hwan Kim

* Corresponding author. Tel.: +1 647 637 3593, Fax.: +1 416 978 0640

E-mail address: smkim@mie.utoronto.ca

© KSME & Springer 2008

for the majority of microassembly. To date, most serial microassembly tasks are manually performed; however, how to achieve automation of such tasks is a necessary step towards creating financially viable microassembly techniques. Therefore, automation of the tasks of 3-D micro-grasp and micro-joining, the subject of this paper, forms the most basic and indispensable component subtasks required for the ultimate success in the automation of MEMS microassembly.

Studying the literature on automatic serial microassembly, various methods have been proposed, which may be divided into two categories, vision-based approaches and force-sensor-based approaches. For the former, Codourey, et al. [7], Kasaya, et al. [8], and Nelson, et al. [9] proposed to use high precision actuators and vision feedback to execute microassembly. For the latter, Zesch and Fearing [10], Sitti and Hashimoto [11] proposed to use force sensors. Recently, with substantial improvement of computer processing power that reflects on increasing image processing speed, much effort has been applied to vision-based microassembly techniques. However, automated microassembly of micron scale components remains an open research field.

In this paper, a new vision-based control strategy for automatic 3-D micro-assembly tasks has been proposed. In the vision control scheme, with respect to micro-grasping and micro-joining sub-tasks, two two-stage motion strategies are employed and the relevant vision control software is developed. Experiments conducted on the experimental MEMS robotic workstation demonstrate the validity of the proposed control approach and the two-stage motion

This paper is organized as follows. Section 2 describes the mechanical structure of the 6-DOF robotic workstation, the video microscope system, the structures of the microgripper, the micropart, and the base structure. Section 3 addresses the proposed vision-based control approach and two two-stage motion strategies. Section 4 shows the experimental results. Finally, Section 5 offers a conclusion to this paper.

2. Robotic workstation, video microscope system, microgripper, micropart and base structure

2.1 6-DOF robotic workstation

In this research, a 6-DOF robotic workstation, with a video microscope system, designed and assembled

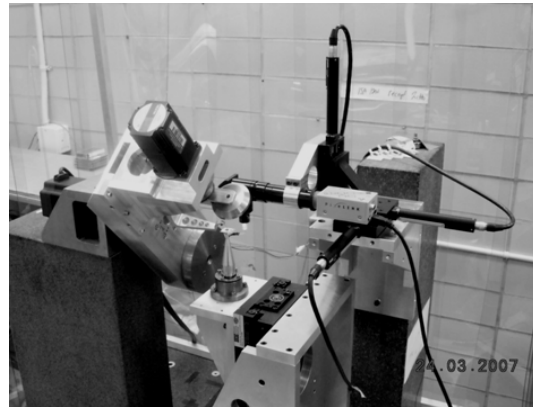


Fig. 1. Detail of 6-DOF MEMS robotic workstation.

by Dechev et al. [3], is used to automatically perform 3-D microassembly tasks. The MEMS robotic workstation, as shown in Fig. 1, is able to simultaneously rotate and translate microparts with respect to the MEMS chip in three rotational DOF (α , β and γ) and three translational DOF (x , y and z) directions. The rotation axes of each of the three rotational joints pass through a common point in space, regardless of the rotational orientation of any of the three axes. During microassembly, this common point in space coincides with the tip of the end-effector, to which a microgripper is bonded. The x , y , z translation axes and the α rotational axis are mounted on a granite base; while the β and γ axes are mounted on a granite post. The robotic workstation has six stepper motors, each driving one axis independently. The stepper motors, providing a rotational resolution of 0.072 deg/pulse, were selected to drive the three rotational axes. The x , y and z axes are driven by ball-bearing lead screws with a 2 mm lead. Combined with the stepper motors, this provides a linear stepper displacement of 0.5 μm .

2.2 Video microscope system

A video microscope system is the primary feedback source of automatic microassembly. As shown in Fig. 2, this system is based on a Nikon CFI60 L Plan Epi 20X objective lens, whose depth of focus is 1.5 μm , and a co-axial illuminator connected in-line with the optics to provide illumination of the MEMS chip. A high bright green LED (light-emitting diode) is used. The optical resolution of whole system is approximately 0.9 μm based on the Rayleigh criterion. The video camera used is a digital, monochrome unit with a 2/3" CCD and a resolution of 1280×1024 pixels.

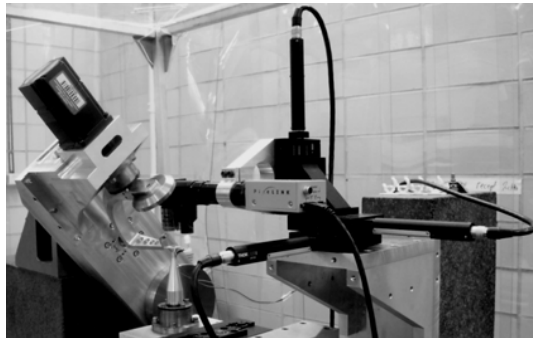


Fig. 2. Video microscope system.

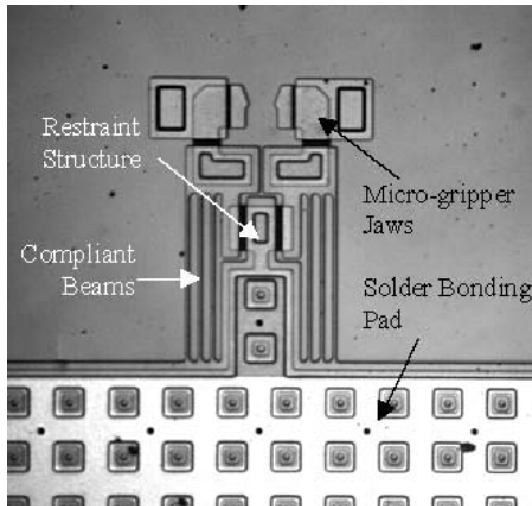


Fig. 3. Passive micro-gripper.

Combined with the microscope system, the resulting field of view is $427H \times 320V$ microns. This microscope system is mounted on an independent 3-axis translation stage, which is controlled by three-step motors, with a lead screw pitch of 0.5 mm. Each stepper motor (model #ZST25) controls one translation direction of the microscope. This allows the microscope to be moved independently of the robot axes, and to be controlled automatically.

2.3 Microgripper, micropart and base structure

The assembly task in this research is performed by using a passive microgripper that is bonded to the tip of the probe, connected to the distal link of the MEMS robotic workstation. In automatic micro-grasping operations, jaws of the bonded microgripper, as shown in Fig. 3, are expected to grasp the body of a designated micropart, as shown in Fig. 4, break two

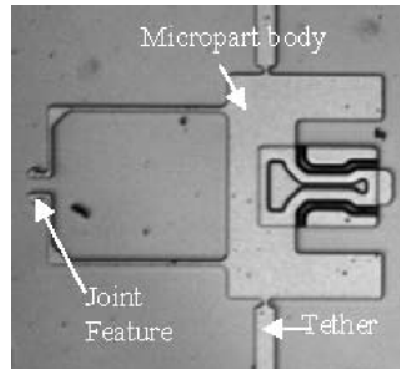


Fig. 4. Micropart.

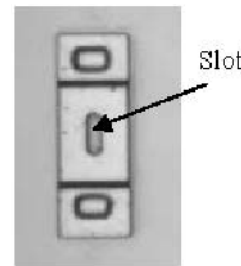


Fig. 5. Base Structure

tethers, and remove the micropart from where it is fixed to the MEMS chip. Fig. 5 shows the base structure, in which the joint of the micropart is expected to be inserted.

The dimension of the micro-gripper, without the bonding pad, is $154 \mu\text{m} \times 88 \mu\text{m}$; the dimension of the micro-part, without tethers, is $160 \mu\text{m} \times 88 \mu\text{m}$; the dimension of base structure is $10 \mu\text{m} \times 58 \mu\text{m}$. All of the microgripper, microparts and base structures are fabricated from polysilicon.

3. Automatic 3-D microassembly strategy

3.1 Overview of the 3-D microassembly process

A typical 3-D microassembly task mainly consists of two sub-tasks: (i) micro-grasping, i.e., to control a passive microgripper to grasp a designated micropart fixed to the MEMS chip, and to break it from the fixing tethers; (ii) micro-joining, i.e., to pivot the grasped micropart, and then join it into a designated slot on the MEMS chip. To perform these two sub-tasks automatically while guaranteeing operation accuracy, different two-stage motion control strategies are employed, with the use of vision-based control.

3.2 Automatic micro-grasping

A flow chart illustrating the automatic micro-grasping process is shown in Fig. 6. The blocks enclosed by the dashed-line represent the manual tasks required to be operated prior to automatic grasping, where x_T and x_G denote the distances between the centre of the patterns of the micropart and the microgripper in the x axis when the microgripper is $5 \mu\text{m}$ from the mating edge of the micropart, and completely grasps the micropart, respectively. Note that the two patterns are selected as a portion of the corresponding microstructures, for the convenience of pattern matching performed by vision control software developed by LabVIEW. The remaining blocks in Fig. 6 represent the tasks performed automatically.

As shown in Fig. 6, a two-stage motion strategy is employed to grasp the micropart. In Stage I, after the patterns of the microgripper and micropart are matched, the relative distances between the centers of the two microstructures in the x and y axes, Δx and Δy ,

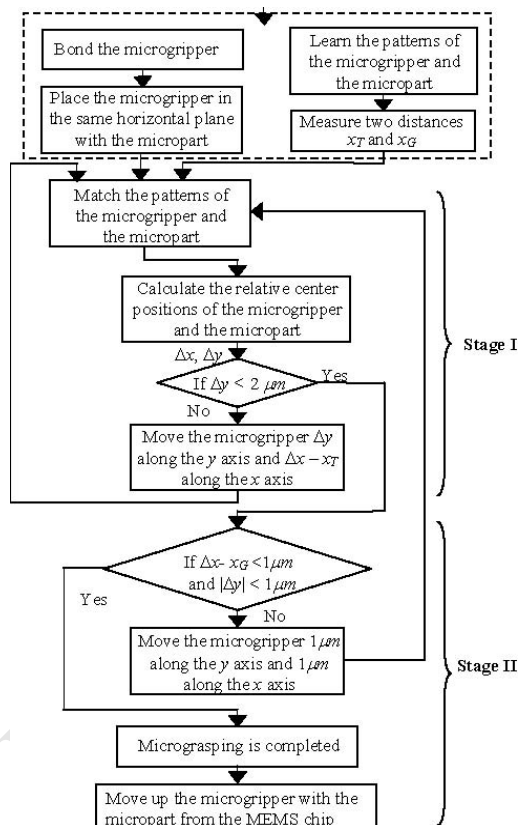


Fig. 6. Flow chart of the micro-grasping.

are calculated. Then the microgripper is translated in the plane to align with the designated micropart, at a distance of $5 \mu\text{m}$ from the mating edge of the micropart. Such a separation avoids the possibility of the microgripper being damaged during the next grasping motions in case the orientations of the two microstructures are not identical. Here, patterns are only matched once. In Stage II, after the patterns of the microgripper and the micropart are matched, the microgripper is displaced towards the micropart in $1 \mu\text{m}$ steps, while maintaining the alignment of the two microstructures in y direction. Such operations are iterated, until $\Delta x - x_G < 1 \mu\text{m}$ and $|\Delta y| < 1 \mu\text{m}$ are satisfied, implying that the micropart has been completely grasped. Then the micropart is broken from the tethers by keeping moving the MEMS chip towards the microgripper. Finally, the microgripper is moved up with the grasped micropart along the z axis.

3.3 Automatic micro-joining

The automatic micro-joining process includes the following operations: translating the grasped micropart to the top of the designated base structure; pivoting the micropart; inserting the tips of the micropart into the slot of the base structure; and releasing the micropart, as shown in Fig. 7. In this flow chart, two preparation works are automatically performed prior to the micro-joining. With the assistance of the CAD model of the MEMS chip, the grasped micropart is translated in a horizontal plane to the top of the designated base structure. Then the micropart is pivoted around the β axis 100 deg so that its tips can be observed clearly in the following step of tips autofocus. Since the micropart is near the common point of the workspace of the robotic workstation, as addressed in Section 2, after rotation, the micropart remains in the microscope's field of view. The following steps of locating the tips of the micro-part and aligning the joint features are crucial to the success of automatic micro-joining operations. We will introduce them in the following two sections.

3.4 Localization of the pivoted micropart in 3-D

Automatically locating the pivoted micropart is a key step in automatic micro-joining. In order to accurately obtain the center positions of the tips of the micro-part in 3-D space, the following strategy is employed. First, the MEMS chip is placed $400 \mu\text{m}$

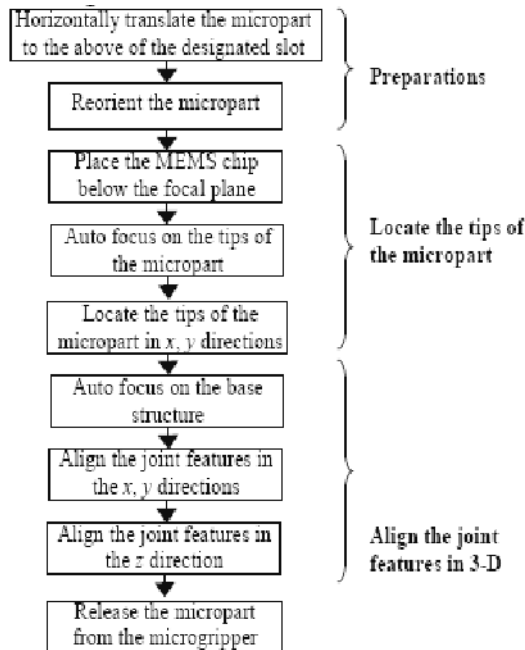


Fig. 7. Flow chart of the micro-joining.

lower than the focal plane of the microscope. Such a distance makes sure that the MEMS chip provides a bright, uniform and steady illumination for the pivoted micropart. The tips of the micropart are on the top of the focal plane. The microscope and the chip are controlled to move up along the z axis with a step of $1\ \mu\text{m}$, simultaneously. At the end of each step, the focus value is calculated by applying a Prewitt filter [12]. When the tips of the micropart appear in the field of view, the focus value generates a step change. Comparing with the focus value with a pre-defined threshold, the tips can be focused well. Finally, the centre position of the tips (x_t , y_t) is obtained by matching the image with a pattern of the tips.

3.5 Aligning the joint features in 3-D

Automatically aligning the joint features, i.e., inserting the tips of the micropart into the slot of the base structure, is crucial to micro-joining. Fig. 8 shows the cross section of the snap-lock joint features. To align the joint features in 3-D, a two-stage motion strategy is employed: (i) joint features are aligned in the x and y directions; (ii) joint features are aligned in the z direction.

In the first stage, at the beginning, the base structure is below the tips and the focal plane, as addressed

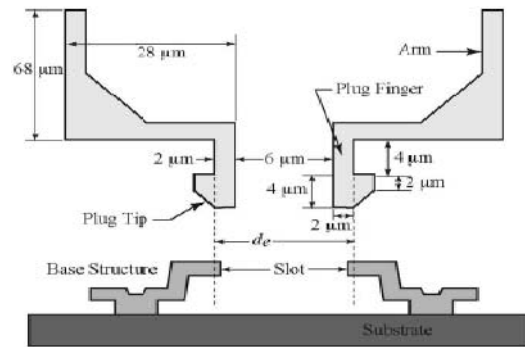


Fig. 8. Cross section of snap-lock joint feature.

in the previous sub-section. Due to in-line illumination in the microscope, the probe casts its shadow on the MEMS chip, which should be eliminated as much as possible to facilitate the following pattern matching. In this paper, the base structure is placed at $900\ \mu\text{m}$ lower than the pivoted micropart in the z direction. As a result, the impact of the shadow on the pattern matching is substantially reduced. Subsequently, the microscope is moved down along the z axis with a step of $1\ \mu\text{m}$ to focus on the base structure by using the same method as focusing on the tips. After focus, through matching the pre-selected base structure pattern, the center position of the designated slot (x_s , y_s) is obtained. The distances between the centers of the joint features in the x and y axis are calculated, and the joint features are aligned in the x and y axis by sending corresponding motion commands

In the second stage, the microscope is moved up along the z axis to re-focus on the tips of the micropart, and then the base structure is moved up until the tips completely insert into the slot. Here, the insertion motion control is performed by using a contact sensor. In this paper, contact detection is performed by using a vision-based method. Due to the structure of the passive snap-lock joint feature, in the insertion process, with the depth of insertion increasing, the gray level of the area around the slot covered by the tips varies substantially. As shown in Fig. 9, before the tips touch the slot, the gray level of the region of interest (ROI), enclosed by the red rectangular, is relatively low. After touching, in the middle of insertion, the gray level has a maximum value. When insertion is completed, and the gray level returns to a lower value. Following this rule, detecting the gray level of ROI can thus be employed to measure the depth of insertion. The peak value of the gray level

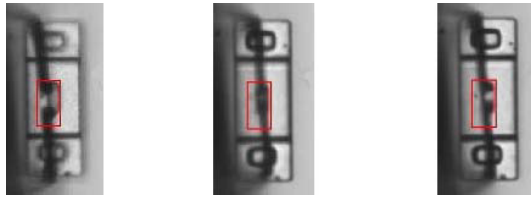


Fig. 9. (a) at the beginning (b) in the middle (c) at the end of insertion.

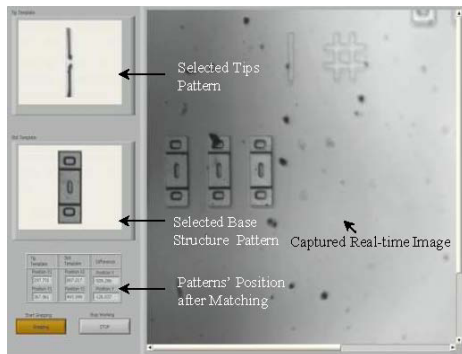


Fig. 10. Interface of the developed vision control software.

that appears in the middle of insertion is easier to detect.

4. Experiments

In order to examine the performance of the proposed vision control strategy and two two-stage motion strategies, experiments of micro-grasping were conducted by using the 6-DOF MEMS robotic workstation and the vision control software developed by LabVIEW, as shown in Fig. 10. Two DMC-1800 Galil cards control the motions of the robotic workstation and the microscope, respectively. The control system is run on a Pentium 4 PC with a 3.4 GHz processor.

Before the 3-D automatic microassembly operations proceed, four operations have to be performed manually, as addressed in Section 3.B. First, the micro-gripper is bonded to the probe tip of the robotic manipulator by applying a UV (ultra-violet) curable adhesive. The microgripper is then manually placed at an arbitrary position adjacent to the micro-part at the same z coordinate, as shown in Fig. 11. The patterns of the microgripper, the micropart, the tips, and the slot are selected. In the end, distance x_T and x_G , as addressed in Section 3.B, $x_T=187.5 \mu\text{m}$, $x_G=147 \mu\text{m}$, are determined. Here, for the patterns of the micropart and the microgripper, we only select a non-

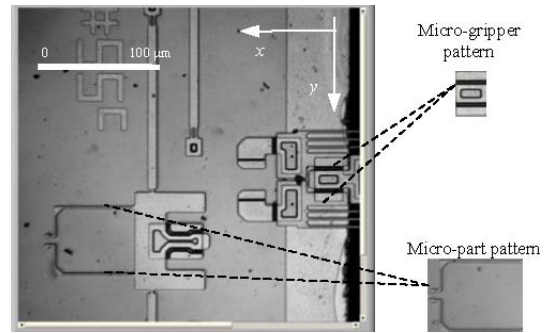


Fig. 11. Patterns of the micro-part and the micro-gripper selected for pattern recognition, to determine the center position of the components.

deformable portion of the corresponding microstructure, for recognition; otherwise, the patterns cannot be matched after the microgripper contacts the micro-part during micro-grasping operations.

After completion of the above preparations, the “run” button on the interface of vision control software is clicked, and automatic micro-grasping is performed first. Through pattern matching, the positions of the microgripper and micropart are obtained as (735.425, 236.864) and (168.56, 421.331) with the unit of pixel, respectively. Here, 1 pixel corresponds to $0.367 \mu\text{m}$. After that, following the two-stage motion strategy introduced in Section 2.B, the bonded microgripper automatically grasps the micropart and removes it from the MEMS chip. Fig. 12(a)–(e) show the whole procedure of micro-grasping operations. Fig. 13 shows the relative displacements of the microgripper with respect to the micropart in the x and y axes. Notably in Stage II, the microgripper moves several microns in the y direction, although the microgripper aligns with the micropart at the end of Stage I. This is because the orientations of the two microstructures are not identical. The whole micro-grasping operations take about 7 sec.

After completion of micro-grasping, the microgripper with the micropart is translated to a place above the designated base structure, and then it rotates 100 deg around the μ axis. Then following the two-stage motion strategy introduced in Section 2.C, the tips of the pivoted micropart are automatically inserted into the slot of the base structure. Fig. 14(a)–(e) show the procedure of micro-joining operations. Fig. 15 shows the jointed 3-D MEMS structure after withdrawing the micro-gripper. Fig. 16 shows a gray value curve when inserting the tips into the slot. The whole micro-joining operations take about 150 sec.

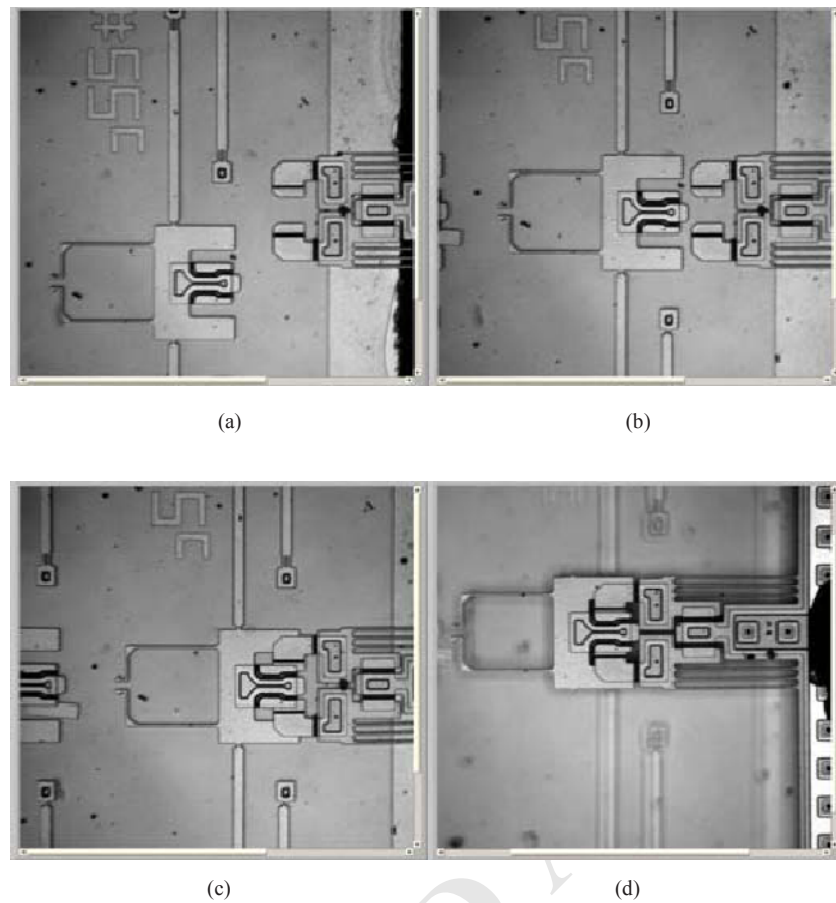


Fig. 12. (a) At the beginning of Stage I, (b) At the beginning of Stage II, (c) In the middle of Stage II, (d) At the end of Stage II

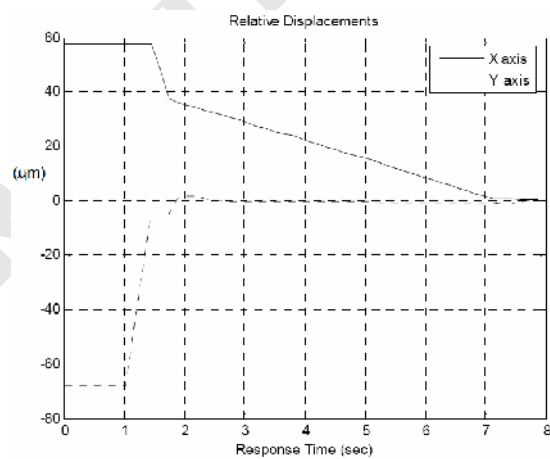


Fig. 13. Relative displacements of the microgripper, w.r.t the micropart.

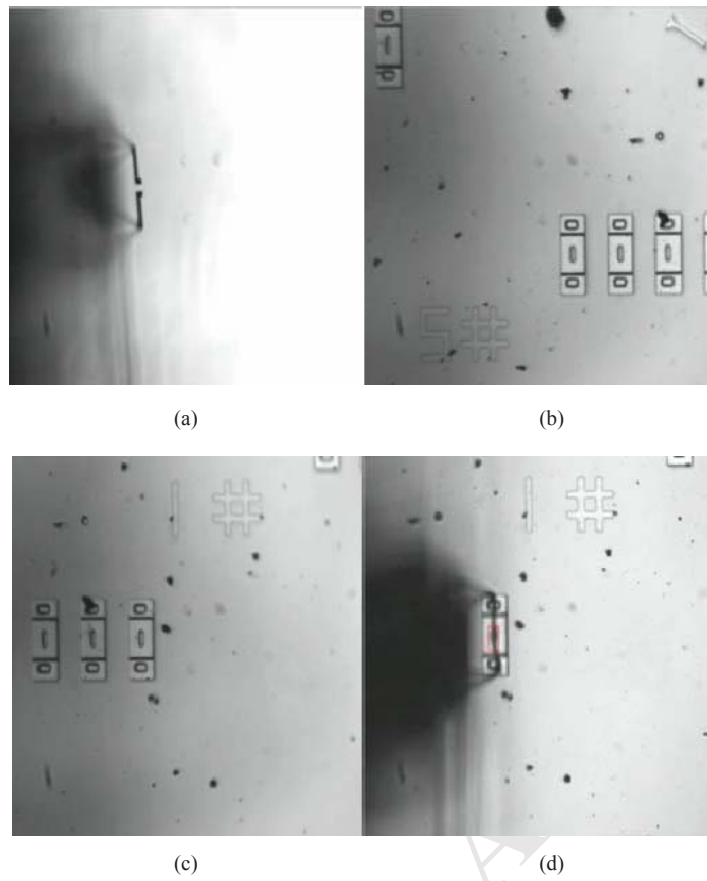


Fig. 14. (a) Locate the tips of micropart, (b) Locate the designated, (c) alignment in the x - y directions, (d) Alignment in the z direction.

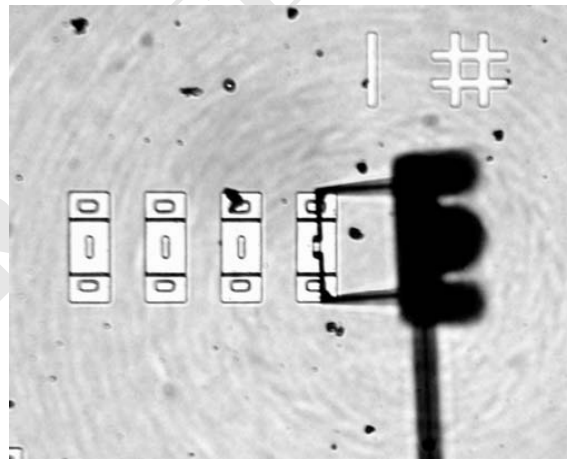


Fig. 15. Jointed 3-D MEMS structure.

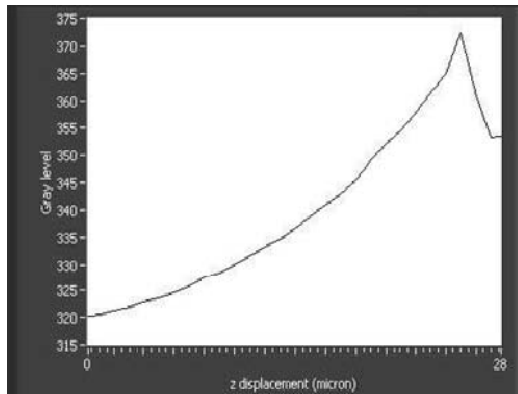


Fig. 16. The gray level curve.

5. Conclusion

We propose a vision-based control strategy to perform 3-D automatic microassembly tasks on a 6-DOF robotic workstation with passive grasping and joining features. Specifically, such microassembly tasks consist of two sub-tasks, micro-grasping, i.e., to control a passive microgripper to grasp a designated micropart fixed to the chip, and micro-joining, i.e., to rotate the grasped micro-part, and then insert it into a designated slot on the chip. In the proposed automatic control scheme, for micro-grasping, a two-stage feedback motion control strategy is employed, where the bonded microgripper is controlled to directly reach a specific position adjacent to matching edge of the designated micropart with the same y coordinate in the first stage, and then the microgripper is controlled to move towards the micropart with steps of 1 μm , until the micropart is completely grasped. Pattern matching is performed only once in the first stage, while being performed at each control iteration in the second stage. For micro-joining, another two-stage motion control strategy is used, with the use of pattern matching and auto-focus. In the first stage, the tips of the pivoted micropart are aligned to the designated slot on the MEMS chip in the x and y directions. In the second stage, the MEMS chip is controlled to move toward the micropart, until the tips are completely inserted into the slot. Here, the depth of insertion is detected by gray value of the interested region around the slot.

References

[1] K. F. Böhringer, R. S. Fearing and K. Y. Goldberg, Microassembly, In Shimon Nof, editor, *The Hand-*

book of Industrial Robotics (2nd edition), John Wiley & Sons, February (1999) 1045.

- [2] Jae Won Choi and Young Myoung Ha, Design of Microstereolithography system Based on dynamic Image Projection for Fabrication of Three-Dimensional Microstructures, *KSME International Journal* 20 (12) (2006) 2094-2104.
- [3] N. Dechev, L. Ren, W. Liu, W. L. Cleghorn and J. K. Mills, Development of a 6 degree of freedom robotic micromanipulator for use in 3D MEMS microassembly, *Proc. of IEEE Int. Conf. on Robotics and Automation* (2006) 281-288.
- [4] R. Sahai, J. Lee and R.S. Fearing, Semi-Automated Micro Assembly for Rapid Prototyping of a One DOF Surgical Wrist, *Proc. of IEEE Int. Conf. on Intelligent Robots and Systems*, Las Vegas, NV, October. (2003) 1882-1888.
- [5] A. Singh, D. Horsely, M., M. Cohn, A. Pisano and R. Howe, Batch transfer of microstructures using flip-chip solder bonding, *J. of Microelectromech. Systems*, 8(1) (1999) 1882-1888.
- [6] K. F. Harsh, V. M. Bright and Y. C. Lee, Solder self-assembly for three-dimensional microelectromechanical systems, *Sensors and Actuator A*, 77, 1999.
- [7] A. Codourey, W. Zesh, R. Buschi and R. Siegart, A robot system for automated handling in Micro-World, *Proc. of IEEE/RSJ Intelligent Robots and Systems* (1995) 185-190.
- [8] T. Kasaya, H. Miyazaki, S. Saito and T. Sato, Micro object handling under SEM by vision based automatic control, *Proc. of SPIE Conf. on Microrobotics and Micromanipulation* (1998) 181-188.
- [9] B. J Nelson, Y. Zhou and B. Vikramaditya, Sensor-based microassembly of hybrid MEMS devices, *IEEE Control Systems* (1998) 35-45.
- [10] W. Zesch and R.S. Fearing, Alignments of microparts using force controlled pushing, *Proc. of SPIE Conf. on Microrobotics and Micromanipulation* (1998) 148-156.
- [11] M. Sitti and H. Hashimoto, Two-dimensional fine particle positioning using a piezoresistive cantilever as a micro/nanomanipulator, *Proc. of IEEE Int. Conf. on Robotics and Automation*, (1999) 2729-2735.
- [12] National Instruments Corporation Technical Staff, *NI Vision Concepts Manual*, National Instruments Corporation (2005).



Lidai Wang received the B.A. Sc. and M.A.Sc. degree in instrument science and technology from the Tsinghua University, Beijing, China, in 2003 and 2005, respectively. He is currently working toward the Ph.D. degree in mechanical engineering at the

University of Toronto, ON, Canada. His research interests include data fusion, computer vision, robotics, micromachines and control. His M.A.Sc. work involved the development of an inertial measurement unit and data fusion algorithm for use in miniature aerial vehicle. His current research specializes in the automation of robotic microassembly and its application.



Seungmin Kim graduated with Bachelor's degree in Mechanical Engineering (1992), Master's degree in Mechanical Engineering (1996) and completed the Ph.D. degree in Mechanical Engineering (2005) from the Pukyung National University,

Pusan, Korea, specializing in control system design. His research interests have encompassed a number of related areas, including: robotics and automation, motion controls, and mechatronics, design and control of high speed machines, MEMS 3D assembly, MEMS robotic task execution, etc. He works as a post-doctoral researcher at the University of Toronto in Canada from January 2008. Since 2005, he has been with the Mechatronics Examination Team at the Korea Intellectual Property Office, and is now an Assistant Director.